ChemComm

COMMUNICATION

View Article Online
View Journal

Cite this: DOI: 10.1039/c9cc03379c

Received 2nd May 2019,
Accepted 19th August 2019

DOI: 10.1039/c9cc03379c

rsc.li/chemcomm

Cell surface clicking of antibody-recruiting polymers to metabolically azide-labeled cancer cells†

Annemiek Uvyn,‡[a] Ruben De Coen,‡[a] Olivier De Wever,[b] Kim Deswarte,[cd] Bart N. Lambrecht[cd] and Bruno G. De Geest *[a]

Triggering antibody-mediated innate immune mechanisms to kill cancer cells is an attractive therapeutic avenue. In this context, recruitment of endogenous antibodies to the cancer cell surface could be a viable alternative to the use of monoclonal antibodies. We report on antibody-recruiting polymers containing multiple antibody-binding hapten motifs and cyclooctynes that can covalently conjugate to azides introduced onto the glycocalyx of cancer cells by metabolic labeling with azido sugars.

The immune system has evolved to provide several lines of defense against invading pathogens. When mucosal or epithelial barriers are crossed, innate immune mechanisms comprise the second line of defense.[1] Amongst others, these rely on adsorption of antibodies onto a target pathogen surface, thereby triggering complement activation, direct killing by NK cells and phagocytosis by macrophages. The latter two mechanisms directly depend on recognition of the antibody Fc-domains by Fc receptors on the cell surface of NK cells and macrophages.[2] The source of antibodies that bind to a pathogen surface originates from immunization campaigns, acquired immunity due to prior infection by the same pathogens, or by external administration of antibodies as passive immunetherapy. Alternatively, one could exploit the virtually unlimited pool of endogenous antibodies against hapten motifs such as dinitrophenol, rhamnose or α-Gal that are found population-wide in human blood due to pesticide exposure, commensal bacteria in the gut or meat consumption.[3,4]

In the context of cancer immune-therapy, strategies are developed to efficiently recruit such endogenous antibodies from the blood stream to the surface of a target cancer cell to mark this cell for destruction by the innate immune system. Very recently, we demonstrated that constructs composed of multiple hapten motifs installed onto a hydrophilic polymer backbone (termed antibody-recruiting polymers or ARPs) largely outperform monovalent antibody-recruiting constructs comprised of only a single hapten motif.[5]

The way antibody-recruiting hapten motifs are typically installed onto a cancer cell surface is either by non-specific hydrophobic anchoring of a lipid tail to the phospholipid cell membrane,[6] by ligand-receptor mediated recognition[7] or by a combination of the latter with covalent conjugation.[8] Both the latter processes are dynamic. Indeed, lipid motifs are known to be mobile on cell surfaces and can shuttle between cells and bind to hydrophobic pockets of serum proteins, such as albumin, and be carried away by the bloodstream.[9] Ligand-receptor binding is characterized by avidity, meaning that the residence time on a cell surface is limited under highly diluted conditions, especially when using monovalent ligands with an avidity that is typically orders of magnitude lower than monoclonal antibodies.

Hence, covalent ligation to the cell surface could be a viable approach to cope with the above-listed challenges. However, none of the canonical amino acids, nor carbohydrate motifs, exhibits orthogonal reactivity to achieve conjugation to a cell surface only, without random conjugation to abundantly present proteins in the extracellular environment.

In this regard, metabolic labeling of cells with azido sugars is a powerful strategy to introduce azide motifs as 'unnatural orthogonal handles' into the glycocalyx that can selectively be conjugated by cyclooctynes through strain-promoted azide–alkyne cycloaddition (SPAAC),[10] forming a stable triazole bond (Scheme 1).

In this paper we aim to explore in the context of ARPs, the introduction of an unnatural cell surface receptor through metabolic labeling of the glycocalyx with azido sugars. As a proof-of-concept we focus on azido sugars that show no selectivity towards cancer cells. But interestingly, novel glycobiology developments by the Cheng group, have led to the development of a next generation of azido sugars that allow for selective metabolic labeling of cancer cells that over-express specific enzymes.[11] This would allow one to introduce an unnatural cell surface receptor by systemic administration of an

[a] Department of Pharmaceutics, Ghent University, Ghent, Belgium. E-mail: br.degeest@ugent.be
[b] Department of Human Structure and Repair, Ghent University, Ghent, Belgium
[c] Laboratory of Mucosal Immunology and Immunoregulation, VIB Center for Inflammation Research, Ghent, Belgium
[d] Department of Internal Medicine and Pediatrics, Ghent University, Ghent, Belgium

† Electronic supplementary information (ESI) available: Experimental details and additional data. See DOI: 10.1039/c9cc03379c

‡ Both authors contributed equally.

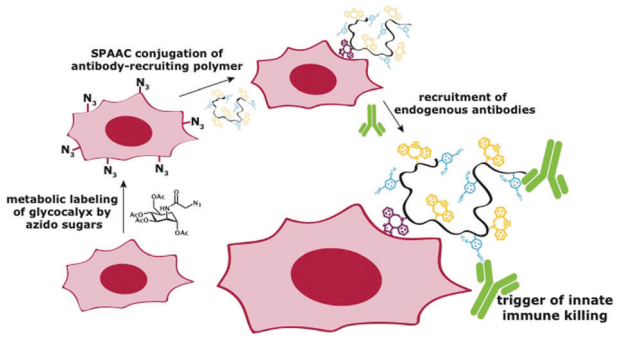

Scheme 1 Antibody recruiting polymer (ARP) concept. First, the glycocalyx of a target cancer cell is engineered with azides by metabolic labeling with an azido sugar. In a second step, ARPs are conjugated to the cell surface by SPAAC between azides in the glycocalyx and cycloalkyne motifs on the ARP backbone. Cell surface conjugation of ARPs triggers recruitment of endogenous antibodies to the cell, thereby flagging the cell for destruction by innate immune effector mechanisms.

azido sugar followed by systemic administration of a cycloalkyne-containing ARP.

We designed ARPs based on an activated ester polymer scaffold that could be subsequently functionalized with SPAAC-reactive and antibody-recruiting motifs. We reasoned that, contrary to the use of polymer with a SPAAC-reactive end-group,[13] multiple of such motifs along a polymer backbone could enhance the binding efficiency to metabolically azide labeled cells. Hereto, pentafluorophenyl acrylate (PFPA)[12] was polymerized by reversible addition–fragmentation chain transfer (RAFT),[14] using 2-(butylthiocarbonothioylthio)propanoic acid (PABTC) as chain transfer agent (CTA). A degree of polymerization (DP) of 100 was targeted, followed by removal of the trithiocarbonate RAFT end-group by treatment with an excess of 4,4-azobis(4-cyanovaleric acid) (ACVA). For detection purpose, a biotin-functionalized (CTA) was used, *i.e.* biotin-PABTC. The synthesis route is depicted in Scheme 2A and the polymer properties are summarized in Table 1. Experimental characterization data are listed in the ESI,† section.

Subsequently, biotin-polyPFPA was substituted with an amine-functionalized cycloalkyne, targeting a degree of substitution (DS; number substituted PFP-ester repeating units per 100) of 2 and 5. Among different types of cycloalkynes, dibenzocyclooctyne (DBCO) was chosen based on its optimal balance between reactivity towards azides and inertness towards other groups,[15] in particular nucleophiles. Note that we did not attempt to increase the DS further due to solubility issues given the hydrophobicity of the DBCO moiety. To generate a hydrophilic polymer backbone, all unreacted PFP esters were converted into hydrophilic repeating units by treatment of the polymer with an excess of 2-aminoethanol.

Prior to testing the conjugation of the DBCO-polymers to cells, we first determined an optimal experimental window for metabolic azide labeling and SPAAC conjugation. Hereto, Jurkat T cells (a model human lymphoma cell line) were cultured for 2 days with different concentrations of the azido sugar *N*-azidoacetylmannosamine (Ac_4ManN_3), followed by staining with DBCO-EG_4-Fluor 545, a red fluorescent DBCO conjugate. Confocal microscopy and flow cytometry (Fig. S20, ESI†) revealed a dose-dependent effect of both the azido sugar and the fluorescent DBCO conjugate.

From these data we concluded that a 25 μM concentration of azido sugar is sufficient to achieve good cell surface labeling with excellent availability/reactivity towards SPAAC conjugation. Importantly, confocal microscopy (Fig. S21, ESI†) proved a homogenous density of the fluorescence over the cell surface and absence of non-conjugated cells (*cf.* overlay between fluorescence and transmitted light (TL) channel), which was also confirmed by flow cytometry (Fig. S21, ESI†). These data show that non-specific binding of dye to cells that were not metabolically labeled with azido sugars is negatable. By contrast,

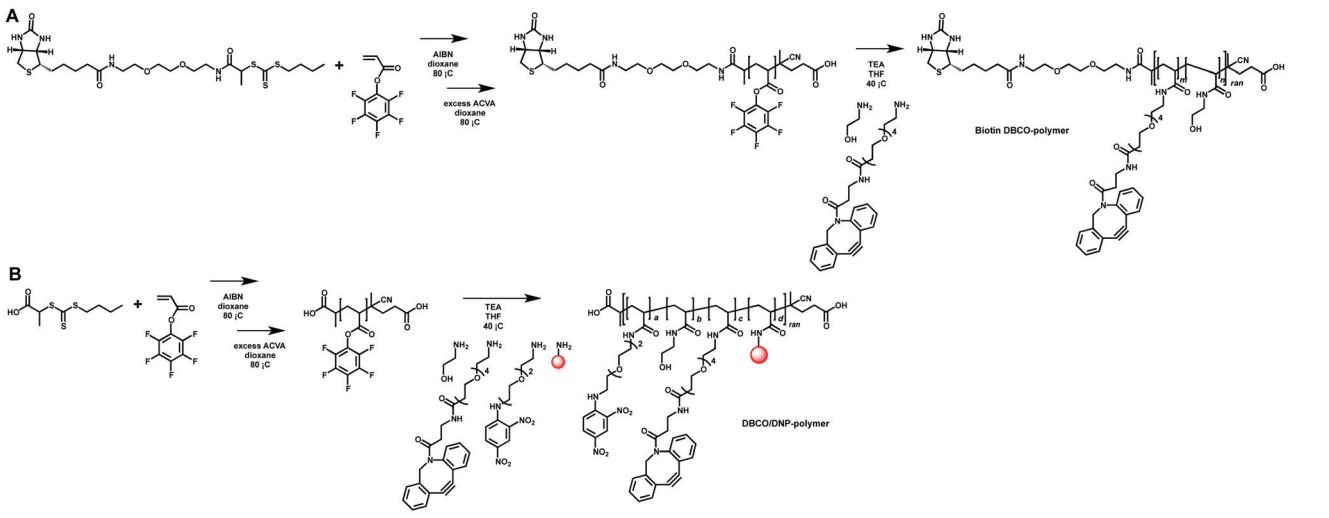

Scheme 2 (A) Synthesis of DBCO-modified polymers by RAFT polymerization followed by trithiocarbonate end-group removal and post-polymerization modification with functional amines. For immobilization or detection purpose, a biotin-functionalized RAFT chain transfer agent was used. Here *m* equals 0,2 or 5 while *n* equals 98, 96 or 93. (B) Synthesis of ARPs with PABTC chain transfer agent composed of DNP and DBCO. Control polymers were synthesized in identical way, but by omitting one or both of the functional amines. Fluorescent labeling was done using rhodamine-cadaverine (represented by a red sphere). Here *a* and *c* equal 0 or 5, *d* equals 1. Therefore *b* equals 74, 79 or 84.

Table 1 Characterization of poly(PFPA) synthesized by RAFT polymerization with (biotin-PABTC) and without biotin-functionalized (PABTC) chain transfer agent

CTA	DP	Conv.[a] [%]	DP[b]	$M_n^{NMR\,b}$ [kDa]	$M_n^{SEC\,c}$ [kDa]	$M_w^{SEC\,c}$ [kDa]	$Đ^d$
Biotin-PABTC	110	89	98	23.9	11.8	15.7	1.33
PABTC	100	85	85	20.5	12.2	14.9	1.22

[a] Conversion determined by ^{19}F-NMR (282 MHz; $CDCl_3$). [b] M_n: number average molecular weight, based on conversion measured by NMR. [c] Determined by SEC (THF), M_w: weight average molecular weight. [d] $Đ$ = dispersity.

azide-labeled cells exhibit a full decade monomodal shift in fluorescence intensity.

Next, we investigated the effect of the DBCO DS on the efficiency of cell surface conjugation. Hereto, cells were cultured in presence of 25 μM of azido sugar, or in absence of azido sugar as control, followed by pulsing with DBCO-polymers and counterstaining with AF488-labeled streptavidin. Flow cytometry (Fig. 1A) showed a highly specific binding of DBCO-polymers to azido sugar labeled cells with an extent of non-specific binding equal to the background fluorescence of the cells. Moreover, DBCO-polymers with a DS of 5 showed greatly enhanced cellular conjugation than DBCO-polymers with a DS of 2, at equal dose of polymer. Confocal microscopy confirmed (Fig. 1B) the flow cytometry data, showing selective binding of DBCO-polymers onto the surface of azido sugar labeled cells.

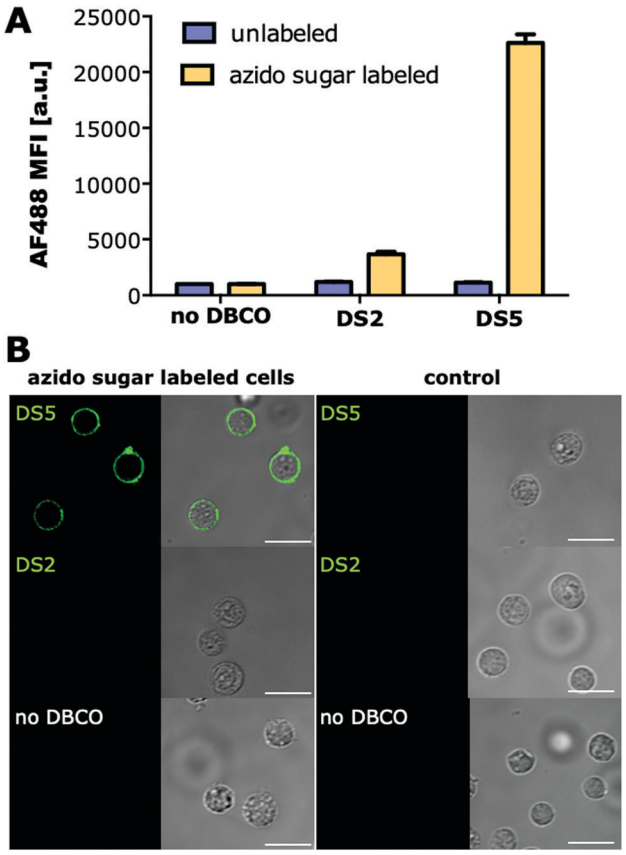

Fig. 1 (A) Flow cytometry analysis (n = 3) and (B) confocal microscopy of Jurkat T cells, with or without metabolic labeling with the azido sugar Ac_4ManN_3, followed by SPAAC conjugation to DBCO-polymers (with biotin end-group). Cells were counterstained with streptavidin-AF488 (green fluorescence). Scale bar represents 10 micron.

Taking into account our observations that DS 5 DBCO-polymers exert selective cell surface binding to azide-labeled cells, we designed ARPs based on a DP 100 polyPFPA backbone substituted with a DS 5 of DBCO and a DS 5 of DNP. Recently, we have demonstrated that a polymer backbone containing 5 DNP units per 100 monomeric repeating units confers an almost 4 log increase in binding avidity to anti-DNP antibodies.[5] This combination also ensures good water-solubility of the resulting polymers as an elevated DNP/DBCO content also increases the overall hydrophobicity. Note that in the context of this work, we elaborated on anti-DNP as a source of endogenous antibodies due to the commercial availability of (fluorescently labeled) anti-DNP antibodies, which strongly facilitates experimental readout compared to the use of full human serum as a source of endogenous antibodies.

A DP 100 polyPFPA polymer was again synthesized by RAFT polymerization using PABTC as CTA. Following trithiocarbonate end-group removal, the polymer was fluorescently labeled with tetramethylrhodamine-cadaverine (DS 1). The polymer was then divided in 4 equal parts and functionalized with DNP and/or DBCO, prior to addition of an excess of 2-ethanolamine. A control polymer without DNP and DBCO was also prepared. The synthesis of these polymers is depicted in Scheme 2B. The reason that we did not use a biotinylated CTA for these experiments was to avoid steric interference between streptavidin binding and anti-DNP recruitment to polymer-treated cells. The polymer properties are summarized in Table 1, while experimental characterization is shown in the ESI,† section.

To test the *in vitro* ability of these polymers to recruit antibodies to the surface of metabolically azide-labeled cells, cells were cultured in the presence of azido sugar and pulsed with different concentrations of the polymers. We first confirmed (Fig. S22, ESI†) that the presence of DNP on the polymer backbone does not impair the ability of the polymers to bind through SPAAC to azido sugar labeled cells. To investigate the antibody-recruiting properties of these polymers, polymer treated cells were washed to remove unbound polymer, followed by pulsing with AF488-labeled anti-DNP antibodies and analysis by flow cytometry. Fig. 2A unambiguously demonstrates that only polymers that contain both DBCO and DNP are capable to recruit antibodies to the cell surface. Importantly, control cells that were not cultured with azido sugar, did neither bind polymer nor antibody. These findings indicate high selectivity of DBCO/DNP-polymers towards azides on the cell surface and low non-specific binding. Confocal microscopy (Fig. 2B) provides further proof of the presence of AF488-labeled anti-DNP on the cell surface of azide-labeled cells treated with DBCO/DNP-polymers but not in any of the controls.

To test whether this approach also holds potential for antibody recruitment in a context of solid tumors, we made use of tumor spheroids that are 3D spherical structures that represent an *in vitro* mimicry of a solid tumor. As cancer cell line we made use of mouse 4T1 cells which is a triple negative breast cancer

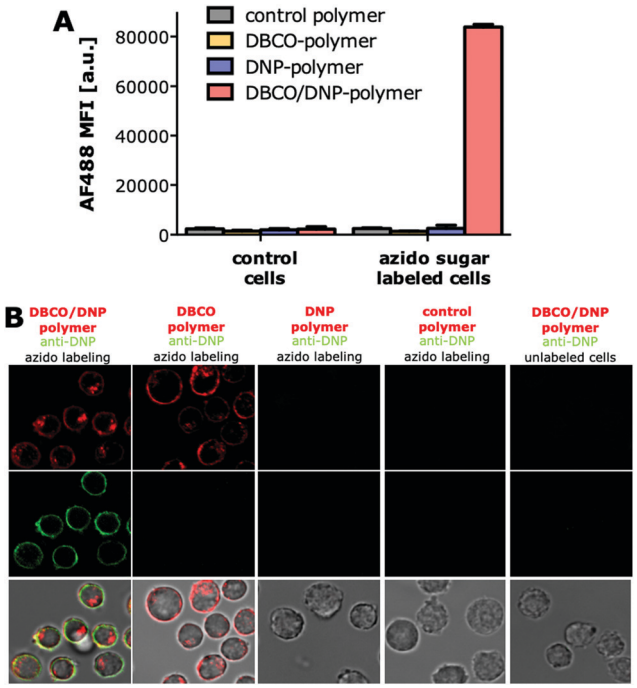

Fig. 2 (A) Flow cytometry analysis of anti-DNP antibody recruitment to azido sugar labeled cells pulsed with polymers. For both cases, non-labeled cells were used as control. (n = 3) (B) Corresponding confocal microscopy images. Red fluorescence (polymer) and green fluorescence (AF488-anti-DNP) are shown separately together with the overlay of both fluorescence channels and the transmitted light (TL) channel.

cell line and also categorized as a so-called 'cold tumor' which shows *in vivo* low infiltration of immune cells under steady state conditions. Hence, strategies that can alter the inflammatory state in the tumor microenvironment, such as antibody-mediated innate responses triggered by ARP binding to tumor cells might be of great relevance. Spheroids were grown and cultured for 48 h with azido sugar prior to addition of ARPs and anti-DNP antibody. Spheroids grown in absence of azido sugar were used as control. Confocal microscopy (maximum intensity projections are shown in Fig. 3, z-stack in Fig. S23, ESI†) show that ARPs show good penetration into the azide-labeled spheroids and bind to the surface of individual cells, whereas only a minor fraction of non-specific binding is observed for spheroids that were not treated with azido sugar. Furthermore, massive anti-DNP binding was observed to the spheroids surface, again with high selectivity for azide-labeled spheroids.

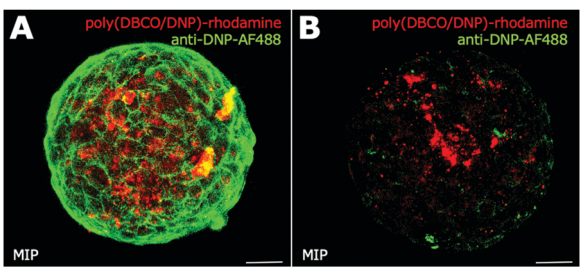

Fig. 3 Confocal microscopy images (maximum intensity projections) of 4T1 mouse breast cancer spheroids, cultured with (A) or without (B) azido sugar and treated with DCBO/DNP-polymer (red fluorescence) and AF488-anti-DNP (green fluorescence). Scale bar represents 50 micron.

One could argue on the limited penetration depth of the antibodies. However, the ARP approach relies on the use of endogenous antibodies that are thus continuously replenished from the blood stream which can be considered as an unlimited source of antibody, compared to administration of a single dose of monoclonal antibody. Hence, strong binding of antibody to the surface of ARP-conjugated tumors is expected to drive potent innate immune effector responses that can then further propagate deeper into the tumor.

In summary, we have demonstrated the ability of polymers containing multiple DBCO moieties as target cell binding motif and DNP moieties as antibody recruiting motif. The feasibility of this approach was demonstrated to be highly efficient on 2D and 3D cell cultures. In our current endeavors we are testing this approach for *in vivo* targeting using cancer cell selective azido sugars and elucidating the innate effector mechanisms involved in cell killing.

This project has received funding from the European Research Council (ERC) under the European Union's Horizon 2020 research and innovation programme (grant agreement No. 817938).

Conflicts of interest

There are no conflicts to declare.

References

1 A. Iwasaki and R. Medzhitov, *Science*, 2010, **327**, 291–295.
2 A. Pincetic, S. Bournazos, D. J. DiLillo, J. Maamary, T. T. Wang, R. Dahan, B.-M. Fiebiger and J. V. Ravetch, *Nat. Immunol.*, 2014, **15**, 707–716.
3 P. J. McEnaney, C. G. Parker, A. X. Zhang and D. A. Spiegel, *ACS Chem. Biol.*, 2012, **7**, 1139–1151.
4 C. E. Jakobsche, C. G. Parker, R. N. Tao, M. D. Kolesnikova, E. F. Douglass and D. A. Spiegel, *ACS Chem. Biol.*, 2013, **8**, 2404–2411.
5 A. Uvyn, R. De Coen, M. Gruijs, C. W. Tuk, M. van Egmond and B. G. D. Geest, *Angew. Chem., Int. Ed.*, DOI: 10.1002/anie.201905093.
6 R. T. C. Sheridan, J. Hudon, J. A. Hank, P. M. Sondel and L. L. Kiessling, *ChemBioChem*, 2014, **15**, 1393–1398.
7 A. F. Rullo, K. J. Fitzgerald, V. Muthusamy, M. Liu, C. Yuan, M. Huang, M. Kim, A. E. Cho and D. A. Spiegel, *Angew. Chem., Int. Ed.*, 2016, **55**, 3642–3646.
8 S. Li, B. Yu, J. Wang, Y. Zheng, H. Zhang, M. J. Walker, Z. Yuan, H. Zhu, J. Zhang, P. G. Wang and B. Wang, *ACS Chem. Biol.*, 2018, **13**, 1686–1694.
9 T. Fritz, M. Voigt, M. Worm, I. Negwer, S. S. Müller, K. Kettenbach, T. L. Ross, F. Roesch, K. Koynov, H. Frey and M. Helm, *Chem. – Eur. J.*, 2016, **22**, 11578–11582.
10 N. J. Agard, J. A. Prescher and C. R. Bertozzi, *J. Am. Chem. Soc.*, 2004, **126**, 15046–15047.
11 H. Wang, R. Wang, K. Cai, H. He, Y. Liu, J. Yen, Z. Wang, M. Xu, Y. Sun, X. Zhou, Q. Yin, L. Tang, I. T. Dobrucki, L. W. Dobrucki, E. J. Chaney, S. A. Boppart, T. M. Fan, S. Lezmi, X. Chen, L. Yin and J. Cheng, *Nat. Chem. Biol.*, 2017, **13**, 415–424.
12 A. Das and P. Theato, *Chem. Rev.*, 2016, **116**, 1434–1495.
13 R. F. Thomas, B. Martyn, T. L. Bailey and M. I. Gibson, *ACS Macro Lett.*, 2018, **7**, 1289–1294.
14 C. Boyer, V. Bulmus, T. P. Davis, V. Ladmiral, J. Liu and S. Perrier, *Chem. Rev.*, 2009, **109**, 5402–5436.
15 J. Dommerholt, F. P. F. T. Rutjes and F. L. van Delft, *Top. Curr. Chem.*, 2016, **374**, 16.

